ACS OMEGA

http://pubs.acs.org/journal/acsodf

Article

Thermal, Electrical, and Environmental Safeties of Sulfide Electrolyte-Based All-Solid-State Li-Ion Batteries

Tongjie Liu,* Lenin W. Kum, Deependra Kumar Singh, and Jitendra Kumar*

Cite This: *ACS Omega* 2023, 8, 12411−12417

Read Online

ACCESS | Metrics & More | Article Recommendations | Supporting Information

ABSTRACT: The next generation of all-solid-state lithium-ion batteries (ASLIBs) based on solid-state sulfide electrolytes (SSEs) is closest to commercialization. Understanding the overall safety behavior of SSE-ASLIBs is necessary for their product design and commercialization. However, their safety behavior in real-life situations, such as battery exposure to high temperature, overcharge, mechanical rupture, and air exposure, remains largely unknown. Herein, we report preliminary but needed evidence of (i) significantly improved resistance to electrical shorting at high temperatures, (ii) reduced heat generation when subjected to excessive heat, (iii) tolerable harmful gas generation when subjected to air exposure followed by high-temperature heating, and (iv) high-voltage charge stability when a battery is overcharged (5.5 V charge) in SSE-based ASLIBs compared to commercial liquid electrolyte-based LIBs (LE-LIBs). Furthermore, the result shows that SSEs can self-induce a fast and effective battery shut-down capability in ASLIBs and avoid thermal runaway upon mechanical damage and exposure to air.

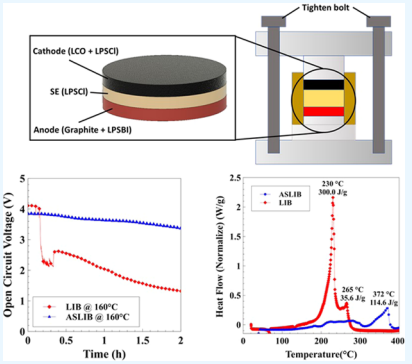

INTRODUCTION

In the last few years, widespread advancements in lithium-ion battery (LIB) technology have accelerated the commercialization of battery-powered electric vehicles.[1,2] Such batteries need to satisfy far more challenging requirements, for instance, high-energy density, faster charge−discharge cycles, safety, long cycling life, etc. Among these, one of the most vital issues in LIBs, which still needs significant improvement, is their overall safety. In this respect, all-solid-state LIBs (ASLIBs) utilizing nonflammable solid-state electrolytes (SEs) are considered promising alternatives to conventional LIBs using flammable organic liquid electrolytes (LEs). As the system becomes LE-free, these ASLIBs are expected to release less energy, resist electrical shorting, and generate minimal harmful gases when damaged or subjected to harsh conditions responsible for thermal runaway.[3−5]

Many inorganic compounds have been explored as SEs for ASLIBs, such as sulfides, oxides, phosphates, etc.[3,6] However, oxide/phosphate-based SEs are intrinsically safer than sulfide-based SEs (SSEs), as sulfides are low in thermal stability and absorb air moisture to form harmful gases like hydrogen sulfide (H_2S) and carbon monoxide (CO).[7−10] Regardless, SSEs are arguably more practical for high-energy ASLIBs because of their high ionic conductivity and lower grain boundary resistance.[11−16] Moreover, the lower elastic modulus of these SSEs results in intimate contact with the active materials when pressed.[17] It allows the fabrication of bulk-type ASLIBs without using sluggish physical vapor deposition techniques needed for fabricating thin-film oxide/phosphate-based ASLIBs. Among SSEs, lithium thiophosphates (Li_3PS_4) and argyrodites (Li_6PS_5X (X = Br, Cl, I)) show high room temperature ionic conductivity ∼1 mS/cm and low interfacial resistance between the electrode/electrolyte, along with easy compressibility, all necessary properties to build commercial-type high-energy cells.[18−20] Therefore, the current research and development activities in building commercially relevant ASLIBs focus on employing lithium thiophosphates/argyrodites as SSEs.

Intensive research on SSE-ASLIBs has been on enhancing their electrochemical performance; however, understanding their operational safety at component and cell levels is still lacking.[21] Therefore, in this work, we present preliminary but essential information about the overall safety behavior of ASLIBs using two SSEs (LPSCl and LPSBI). These two SSEs are used because LPSBI has a higher ionic conductivity and anode stability.[18−20] In contrast, LPSCl has relatively higher stability against high-voltage cathodes, such as lithium cobalt oxide ($LiCoO_2$, LCO), lithium nickel manganese cobalt oxide, etc., which require charging at higher voltages (>4 V).[22] We have investigated the thermal, electrical, and environmental safeties of ASLIBs consisting of a (i) LPSCl + LCO cathode, (ii) LPSCl electrolyte, and (iii) LPSBI + graphite anode and compared the data with LE-LIBs. Differential scanning calorimetry (DSC) has been used to determine thermal safety. Temperature-dependent changes in the open circuit voltage (OCV) of fully charged cells

Received: January 13, 2023
Accepted: March 3, 2023
Published: March 21, 2023

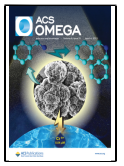

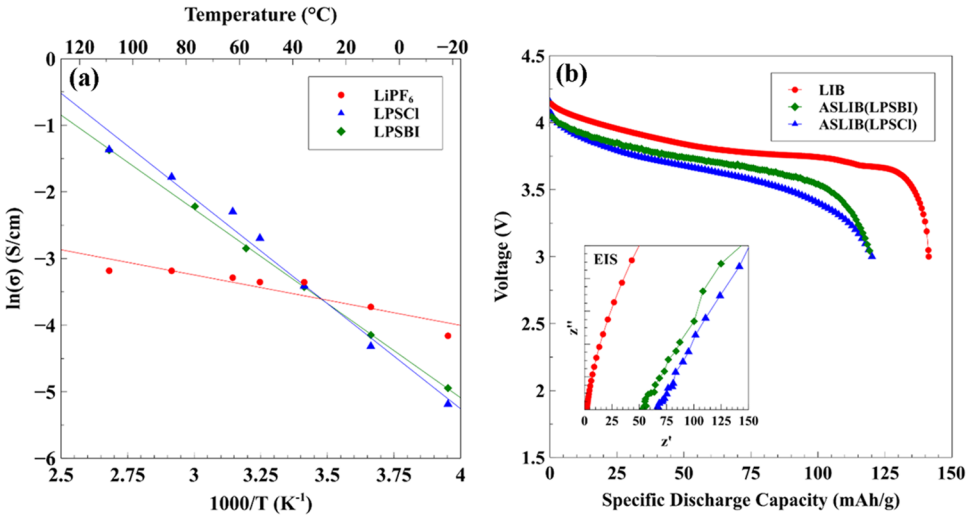

Figure 1. (a) Arrhenius plots of SSEs (LPSCl, LPSBI) and LE (1 M $LiPF_6$ in EC:DMC:EMC +2 wt % VC). (b) Discharge curves of ASLIBs using LPSCl (blue curve) and LPSBI (green curve) vs LE-LIBs (red curve). Inset (panel (b)) shows impedance (Nyquist) plots of ASLIBs using LPSCl (blue curve) and LPSBI (green curve) electrolytes vs LE-LIBs (red curve).

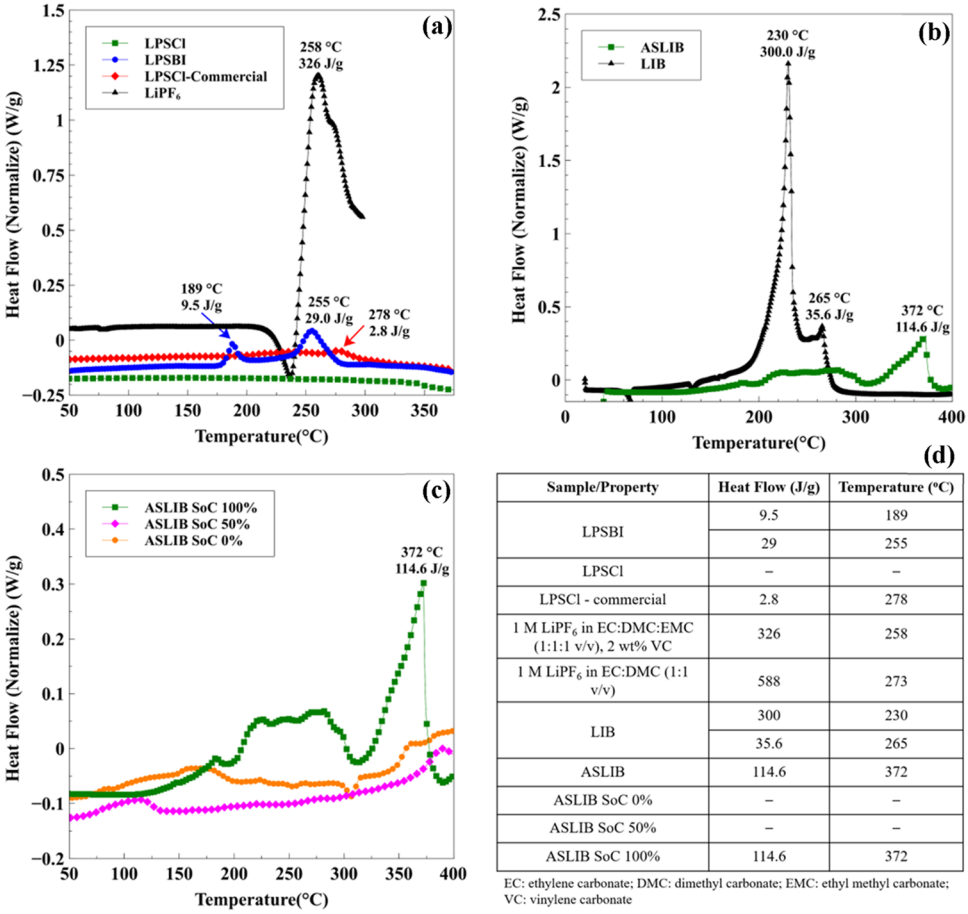

Sample/Property	Heat Flow (J/g)	Temperature (°C)
LPSBI	9.5	189
	29	255
LPSCl	–	–
LPSCl - commercial	2.8	278
1 M $LiPF_6$ in EC:DMC:EMC (1:1:1 v/v), 2 wt% VC	326	258
1 M $LiPF_6$ in EC:DMC (1:1 v/v)	588	273
LIB	300	230
	35.6	265
ASLIB	114.6	372
ASLIB SoC 0%	–	–
ASLIB SoC 50%	–	–
ASLIB SoC 100%	114.6	372

EC: ethylene carbonate; DMC: dimethyl carbonate; EMC: ethyl methyl carbonate; VC: vinylene carbonate

Figure 2. DSC curves of the (a) different electrolytes, (b) LE-LIB and SSE-ASLIB full cells, and (c) SSE-ASLIB at different SoCs. (d) Table summarizing all of the DSC parameters obtained from the plots shown in panels (a–c).

have been done to determine electrical safety. ASLIB cells at different states of charge (SoCs) have been exposed to air and heated at high-temperature (23–500 °C) in the air to determine their environmental safety by quantifying released H_2S due to thermal decomposition. A mechanism has been observed that can quickly shut down the cell operation upon mechanical damage to the cell and the resultant air exposure—an in-built safety valve in SSE-based ASLIBs is necessary to mitigate battery thermal runaway. In liquid electrolyte-based Li-ion batteries, polymer separator shut-down is a safety mechanism to avoid battery thermal runaway.[23]

https://doi.org/10.1021/acsomega.3c00261
ACS Omega 2023, 8, 12411−12417

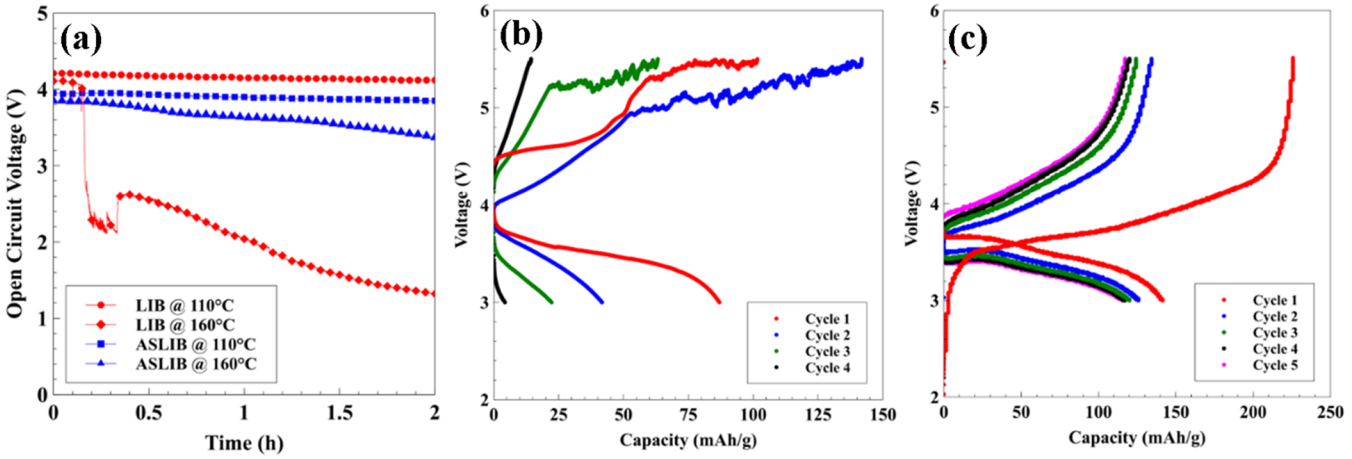

Figure 3. (a) OCV of a charged SSE-ASLIB vs a charged LE-LIB at different temperatures. Voltage vs capacity plots at high-voltage (3−5.5 V) cycles for the (b) LE-LIB and (c) SSE-ASLIB.

RESULTS AND DISCUSSION

Ion Conductivity. We have confirmed the quality of synthesized SSEs (LPSCl and LPSBI) using impedance measurements. From the slope of the Arrhenius plot (Figure 1a), activation energies (E_a) of the two SSEs have been estimated using the equation

$$\sigma(T) = A \exp(-E_a/RT) \quad (1)$$

where T is the absolute temperature, A is a pre-exponential factor, and R is the gas constant. For LPSBI, E_a is 0.24 eV, whereas for LPSCl, E_a is 0.27 eV. Referring to earlier published reports,[24,25] these SSEs can be utilized as SEs for ASLIBs.

Electrochemical behaviors of full cells with SSEs have been studied by constant current charge/discharge cycling at room temperature (RT). Two ASLIBs with an LPSBI and LPSCl SEs, an LCO+LPSCl cathode, and a graphite+LPSBI anode have been cycled along with a LE-LIB having an LCO cathode and a graphite anode. At the second discharge (Figure 1b), the cells with LPSBI, LPSCl, and LE (1 M $LiPF_6$ in EC:DMCEMC +2 wt % VC) exhibited specific discharge capacities of 119.77, 77.59, and 141.31 mAh/g, respectively. The performance corroborated the observation from the Arrhenius (Figure 1a) and the Nyquist (inset of Figure 1b) plots, where it is seen that LE shows a higher conductivity as compared to the SSEs at RT. Based on the Arrhenius plot in Figure 1a, the conductivity of LE is better than SSEs below RT (measured up to −20 °C for this experiment). Hence, the low-temperature performance of LE-LIB is expected to be better than SSE-ASLIB. However, the ASLIBs are expected to perform better at temperatures above RT. Given that these ASLIBs show competitive electrical and electrochemical performances compared to LE-LIBs, we are confident that the safety data generated and analyzed below will have direct commercial significance for the development of ASLIBs.

Thermal Safety. Thermal runaway is one of the major failure modes in LIBs. Generally, it occurs due to a series of uncontrolled exothermic reactions releasing a large amount of heat, which increases the reaction rate because of the temperature, possibly resulting in an explosion.[26] Thus, it is of utmost importance to investigate the operational range of ASLIBs. The severity of the thermal safety of a battery depends on several factors including, but not limited to, the chemical composition of electrolytes and electrodes,[27] the amount and rate of heat released, heat release initiation temperature, types and the amounts of gases generated during battery heating/fire, etc. For a thermally safe or, more accurately, a thermally *safer*[27] battery, the heat released, if any, should be small enough that it does not initiate any unwanted chemical/exothermic reactions responsible for thermal runaway. Before measurements, the SSE-ASLIB and the LE-LIB were charged to 4.3 V (100% SoC). Figure 2a shows the heat release profiles of the two SSEs, and it is observed that LPSCl is thermally superior to LPSBI. Moreover, the heat released from the LE is much higher than that from SSEs. For example, LPSCl barely releases any heat (Figure 2a - green curve) vs LE (326 J/g at 258 °C (Figure 2a - black curve)). The heat generation and exothermic peak observed in the present work are similar to earlier reported work, showing an exothermic peak at 273 °C with a higher magnitude of heat generated (588 J/g).[28] Therefore, LPSCl is the best choice, in terms of thermal safety, to fabricate ASLIBs.

Figure 2b compares the DSC curves of the fully charged (4.3 V, 100% SoC) SSE-ASLIB and LE-LIB using an LCO cathode and a graphite anode. The conventional LE-LIB starts releasing heat below 200 °C and becomes more energy-intense than SSE-ASLIB, which releases heat ∼300 °C (∼100 °C difference) with lower heat intensity. The LE-LIB also shows two major exothermic peaks at 230 and 265 °C; the corresponding changes in the enthalpy are 300 and 35.6 J/g, respectively. On the other hand, the fully charged SSE-ASLIB shows one exothermic peak at 372 °C, with the corresponding change in enthalpy of 114.6 J/g. Compared to the LE-LIB, the exothermic reaction of the SSE-ASLIB appears at a higher temperature, releasing a small amount of heat. More importantly, the heat release rate is slower. The heat release in the LE-LIB is sharp, a large cell format, which can lead to quick local heating (less time for heat to dissipate) and thermal runaway.

Figure 2c compares the heat release profiles of the SSE-ASLIB at different SoCs. It is found that apart from the cell with 100% SoC, no significant exothermic peaks were observed in the cells with lower SoCs, suggesting that the ASLIB becomes more thermally active as the SoC increases. In contrast, the heat released (above 300 °C) in the ASLIB is gradual, minimizing the probability of local heating by improving the chance of more natural heat dissipation. Thus, these results confirm that the SSE-based LIBs are thermally more stable and safer than the conventional LIBs and can be used even for higher temperature operations.

https://doi.org/10.1021/acsomega.3c00261
ACS Omega 2023, 8, 12411−12417

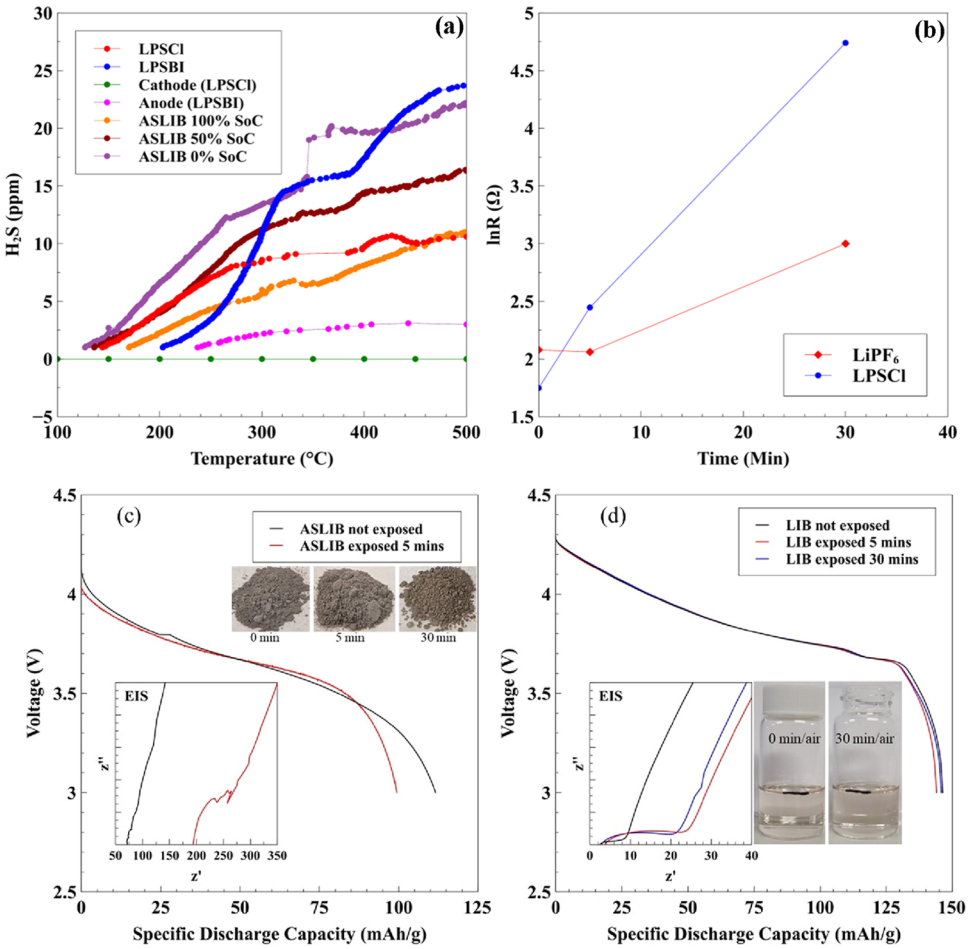

Figure 4. (a) Air stability of SSEs and SSE-based ASLIBs, represented by H_2S release with increased temperature changing, with different SoCs, (b) resistance change of the LE and SSE vs the time of air exposure, (c) discharge and resistance of ASLIBs and color change of the SSE before and after air exposure, and (d) discharge and resistance of LE-LIBs and color change of the LE before and after air exposure.

Electrical Safety. Another critical failure mode in LIBs is electrical shorting, either due to dendrite formation in an aged cell or the separator's mechanical failure (rupture/melting) at high temperatures. An electrical short can cause high current flow internally in the cell that leads to battery heating, causing damage to the separator, electrolyte, and consequently, damage to the electrodes, eventually resulting in battery thermal runaway. One of the plausible solutions to this problem is to replace the low melting separator used in the LE-LIB with an SE.[29,30] Figure 3a shows the variation in the OCV of the SSE-ASLIB and LE-LIB at different temperatures. At 110 °C, the OCV of a fully charged LE-LIB gradually decreases in 2 h, whereas, at 160 °C, the OCV significantly drops down after 500 s and keeps falling at a much higher rate when compared to the OCV, decreasing at 110 °C. This may be ascribed to the shrinkage of the polyethylene separator at high temperatures.[23]

A sudden voltage drop can be the signature of the direct electrical shorting of a battery. As high temperatures accelerate chemical degradation, the marginal voltage drop is also expected in ASLIBs.[21] As shown in Figure 3a, the SSE-ASLIB exhibits a slow voltage drop at 160 °C; notably, the voltage drop is not as rapid as in the LE-LIB. The dimensional stability of the SSE (LPSCl, annealing temperature 550 °C) prevents direct electrical shorting of ASLIBs even at higher temperatures. Thus, this small loss in voltage in the ASLIB can be attributed to the chemical degradation of the electrolyte/electrode at high temperatures such as 160 °C. Hence, the SSE system present in ASLIBs can resist electrolyte-led electrical shorting even beyond 160 °C and is expected to eliminate or delay the thermal runaway.

Yet another battery failure mode that can initiate thermal runaway is charging the LIB to higher voltages. For example, in a LE-LIB with an LCO cathode, irreversible structural changes and cobalt dissolution happen if it is overcharged. Overcharge can cause unstable charge voltage (formation of microshorts) and fast decay of discharge capacity.[31] Figure 3b shows the first 4 cycles of a LE-LIB, which has been charged/discharged to 5.5/3 V. Significant discharge capacity decay can be observed after each cycle; the specific discharge capacity of the 4th cycle is 10.3% of the 2nd cycle. In contrast, after the first cycle of the solid electrolyte interphase formation, the following 4 cycles show a very minute capacity decay despite the fact that the ASLIB has been repeatedly charged to 5.5 V and discharged to 3 V (Figure 3c). The specific discharge capacity of 4th cycle is 93.2% of the 2nd cycle. Moreover, even after repeated overcharging to 5.5 V, the voltage profile of the ASLIB remains stable, unlike microshorts observed in the LE-LIB. This demonstrates the ability of ASLIBs to sustain repeated high-voltage charges and hence embodies high electrical safety compared to LE-LIBs.

Environmental Safety. Environmental safety is another parameter that can be critical in determining the usefulness of

https://doi.org/10.1021/acsomega.3c00261
ACS Omega 2023, 8, 12411−12417

these SSEs in commercial batteries. As reported earlier, LE-LIBs can emit several fatal gases, including hydrogen fluoride (HF), when burning.[32] It has been shown that SSEs can react to moist air and form undesirable gases like H_2S.[7,8] Utilizing the exact quantities of the materials used to fabricate the full cells, all measurements for the SSEs and SSE-based components have been carried out. Figure 4a shows the concentration of H_2S released upon the contact of SSEs, SSE-based components, and ASLIBs with air, representing the air stability of SSEs and their derivatives. The observed patterns show that LPSCl has a gradually increasing slope for temperatures lower than 300 °C. The release rate slowed down from 300 to 400 °C, forming a plateau. At 400 °C, the rate of release increases again. Similar behavior is observed in LPSBI with a higher level of H_2S generated, both in the amount and rate of release. Due to negligible amounts of SSEs in the electrodes, the H_2S release is observed only from the anode sample. This result agrees with the observation of LPSBI being less stable than LPSCl. ASLIBs with different SoCs obey the following trend of H_2S release, with the order from high to low: 0, 50, and 100% SoC. The most probable reason for the sudden increase in the H_2S release rate could be the cracking of the ASLIB pellet due to heating that can expose SSEs to air (high temperatures can induce cracks in the cell stack, Figure S1) and lead to a higher rate of H_2S release. The maximum H_2S level detected was <25 ppm, which can cause fatigue, loss of appetite, headache, irritation, poor memory, and dizziness, but not loss of life.

Figure 4b shows changes in SSE (LPSCl) and LE resistances with air exposure time. In the first 5 min, the difference in resistance of LPSCl and LE were (+) 4% and (−) 4.1%, respectively. After 30 min, the change was drastic, especially in LPSCl, with the change in resistance of LPSCl and LE being (+) 981% and (+) 7.3%, respectively. The LE remains conducting for a longer time. In contrast, the SSE decomposes in 30 min air exposure, and its deteriorating electrochemical behavior can further be confirmed at the cell level (Figure 4c,d).

ASLIBs using a 30 min air-exposed SSE could not discharge, and the impedance plot was too scattered to show herein as a comparison. Figure 4c shows a decline in discharge capacity and an increase in impedance of ASLIBs using a 5 min air-exposed SSE. As seen from the inset pictures of Figure 4c, as the time of air exposure increases, the color of the SSE rapidly changes from gray to brown. Also, the particles of the 30 min air-exposed SSE are significantly agglomerated and show a weight gain of 12.5% (weight before air exposure = 88 mg, weight after 30 min air exposure = 99 mg), mainly due to moisture absorption and reaction with oxygen. On the other hand, the LE exposed to air for 5 and 30 min results in a slight increase in impedance, but discharge capacity is largely unaffected Figure 4d. No color change was observed for the LE before and after 30 min air exposure, implying that the LE degrades in the presence of air, but the rate of degradation is too slow compared to air degradation of the SSE.

The data from Figure 4 implies that the resistance increase in the SSE-ASLIB upon air exposure is rapid and can work as a **safety valve** in shutting down Li^+ transport in ASLIBs. Thus, the separator needs to shut down to avoid thermal runaway initiation when the battery is subjected to accidents and is cut open to air. This *self-creating safety-valve* characteristic (quick resistance rise when exposed to ambient air) of the SE is a new observation and can prove vital in ASLIB safety.

CONCLUSIONS

SSE-based ASLIBs show excellent operational safety compared to LE-LIBs. For example, ASLIBs show: (i) less intense and late initiating exothermic peaks, (ii) no electrical shorting beyond 160 °C, (iii) cycling up to 5.5 V charge, (iv) marginal amounts of H_2S when heated up to 500 °C, and (v) a capability of self battery shut-down in case of air exposure. Thus, the results of thermal, electrical, and environmental abuse tests suggest that SSE-ASLIBs are exceptional in terms of safety compared to their LE-based LIB counterparts. We believe the findings of this work would be beneficial for designing and commercializing next-generation high-energy, high-safety ASLIBs suitable to operate in harsh conditions.

EXPERIMENTAL METHODS

The SSEs (LPSCl (Li_6PS_5Cl) and LPSBI ($Li_7P_2S_8Br_{0.5}I_{0.5}$)) have been synthesized in-house in a box furnace inside an argon-filled glove box (Figure S2), using a scalable manufacturing process. The detailed synthesis procedure has been given in the Supporting Information. This modified synthesis/annealing process of SSEs using a furnace differs from the earlier method that involves annealing the SSEs in sealed (volume constraint) quartz tubes.[20] The electrical and electrochemical behavior of the synthesized SSEs have been evaluated by measuring impedance, charge/discharge, and DSC tests. The air exposure test was done in a tube furnace connected to a sealed box with a H_2S and CO sensor and a hygrometer in it (Figure S3). These experimental details have been provided in the Supporting Information. Furthermore, two sets of experiments were designed: (i) LIB using fresh LE, 5 and 30 min air-exposed and (ii) ASLIB using fresh SSE, 5 and 30 min air-exposed, to prove the air safety of SSE-based ASLIBs vs LE-based LIBs. The impedance of all of the cells using fresh and air-exposed electrolytes was measured to determine the extent of electrolyte degradation when exposed to air for both the LE and SSE. The discharge capacities of the LIB and ASLIB using fresh and air-exposed electrolytes were also measured to prove the real-life functional impact of air exposure.

ASSOCIATED CONTENT

Supporting Information

The Supporting Information is available free of charge at https://pubs.acs.org/doi/10.1021/acsomega.3c00261.

Detailed procedure of sintering of electrolytes; H_2S detection set-up in the air exposure experiment; conditions of the pellets before and after the air/temperature exposure experiment (PDF)

AUTHOR INFORMATION

Corresponding Authors

Tongjie Liu − *Solid-State Batteries & Integrated Systems Laboratories, Power & Energy Division, Department of Electrical & Computer Engineering, University of Dayton, Dayton, Ohio 45469-7531, United States*; Email: liut01@udayton.edu

Jitendra Kumar − *Solid-State Batteries & Integrated Systems Laboratories, Power & Energy Division, Department of Electrical & Computer Engineering, University of Dayton, Dayton, Ohio 45469-7531, United States*; orcid.org/0000-0002-2039-4436; Phone: 937-229-5314; Email: Jitendra.Kumar@udri.udayton.edu, Jkumar1@udayton.edu; Fax: 937-229-3873

https://doi.org/10.1021/acsomega.3c00261
ACS Omega 2023, 8, 12411−12417

Authors

Lenin W. Kum − *Solid-State Batteries & Integrated Systems Laboratories, Power & Energy Division, Department of Electrical & Computer Engineering, University of Dayton, Dayton, Ohio 45469-7531, United States;* orcid.org/0000-0003-4401-3228

Deependra Kumar Singh − *Solid-State Batteries & Integrated Systems Laboratories, Power & Energy Division, Department of Electrical & Computer Engineering, University of Dayton, Dayton, Ohio 45469-7531, United States*

Complete contact information is available at: https://pubs.acs.org/10.1021/acsomega.3c00261

Author Contributions

The manuscript was written through the contributions of all authors. All authors have approved the final version of the manuscript.

Notes

The authors declare no competing financial interest.

■ ACKNOWLEDGMENTS

The authors greatly appreciate the financial support from the Federal Aviation Administration (FAA) of the USA under contract no. 692-M15-20-C-00008. For Arrhenius data plotting, T.L. would like to acknowledge Dr. Ashish Gogia, Rivian Automotive. T.L. also thanks the Department of Electrical and Computer Engineering at the University of Dayton for providing an assistantship.

■ REFERENCES

(1) Chen, W.; Liang, J.; Yang, Z.; Li, G. A review of lithium-ion battery for electric vehicle applications and beyond. *Energy Procedia* **2019**, *158*, 4363−4368.

(2) Farmann, A.; Waag, W.; Uwe, D. Application-specific electrical characterization of high power batteries with lithium titanate anodes for electric vehicles. *Energy* **2016**, *112*, 294−306.

(3) Rao, R. P.; Adams, S. Studies of lithium argyrodite solid electrolytes for all-solid-state batteries. *Phys. Status Solidi A* **2011**, *208*, 1804−1807.

(4) Wang, S.; Tang, M.; Zhang, Q.; Li, B.; Ohno, S.; Walther, F.; Pan, R.; Xu, X.; Xin, C.; Zhang, W.; et al. Lithium argyrodite as solid electrolyte and cathode precursor for solid-state batteries with long cycle life. *Adv. Energy Mater.* **2021**, *11*, No. 2101370.

(5) Liu, Y.; Meng, X.; Wang, Z.; Qiu, J. A Li2S-based all-solid-state battery with high energy and superior safety. *Sci. Adv.* **2022**, *8*, No. eabl8390.

(6) Samson, A. J.; Hofstetter, K.; Bag, S.; Thangadurai, V. A bird's-eye view of Li-stuffed garnet-type $Li_7La_3Zr_2O_{12}$ ceramic electrolytes for advanced all-solid-state Li batteries. *Energy Environ. Sci.* **2019**, *12*, 2957−2975.

(7) Nikodimos, Y.; Huang, C. J.; Taklu, B. W.; Su, W. N.; Hwang, B. J. Chemical stability of sulfide solid-state electrolytes: stability toward humid air and binders. *Energy Environ. Sci.* **2022**, *15*, 991−1033.

(8) Cai, Y.; Li, C.; Zhao, Z.; Mu, D.; Wu, B. Air stability and interfacial compatibility of sulfide solid electrolytes for solid-state lithium batteries: Advances and Perspectives **2022** *9* e202101479 DOI: 10.1002/celc.202101479.

(9) Famprikis, T.; Canepa, P.; Dawson, J. A.; Islam, M. S.; Masquelier, C. Fundamentals of inorganic solid-state electrolytes for batteries. *Nat. Mater.* **2019**, *18*, 1278−1291.

(10) Chen, Y-T.; Marple, M. A. T.; Tan, D. H. S.; Ham, S-Y.; Sayahpour, B.; Li, W-K.; Yang, H.; Lee, J. B.; Han, H. J.; Wu, E. A.; et al. Investigating dry room compatibility of sulfide solid-state electrolytes for scalable manufacturing. *J. Mater. Chem. A.* **2022**, *10*, 7155−7164.

(11) Lacivita, V.; Westover, A. S.; Kercher, A.; Phillip, N. D.; Yang, G.; Veith, G.; Ceder, G.; Dudney, N. J. Resolving the amorphous structure of lithium phosphorus oxynitride (Lipon). *J. Am. Chem. Soc.* **2018**, *140*, 11029−11038.

(12) Li, J.; Ma, C.; Chi, M.; Liang, C.; Dudney, N. J. Solid electrolyte: The key for high-voltage lithium batteries. *Adv. Energy Mater.* **2015**, *5*, No. 1401408.

(13) Sahu, G.; Rangasamy, E.; Li, J.; Chen, Y.; An, K.; Dudney, N.; Liang, C. A high-conduction Ge substituted Li_3AsS_4 solid electrolyte with exceptional low activation energy. *J. Mater. Chem. A* **2014**, *2*, 10396−10403.

(14) Sahu, G.; Lin, Z.; Li, J.; Liu, Z.; Dudney, N.; Liang, C. Air-stable, high-conduction solid electrolytes of arsenic-substituted Li_4SnS_4. *Energy Environ. Sci.* **2014**, *7*, 1053−1058.

(15) Kanno, R.; Hata, T.; Kawamoto, Y.; Irie, M. Synthesis of a new lithium ionic conductor, thio-LISICON-lithium germanium sulfide system. *Solid State Ionics* **2000**, *130*, 97−104.

(16) Kraft, M. A.; Culver, S. P.; Calderon, M.; Bocher, F.; Krauskopf, T.; Senyshyan, A.; Dietrich, C.; Zevalkink, A.; Janek, J.; Zeier, W. G. Influence of lattice polarizability on the ionic conductivity in the lithium superionic argyrodites Li_6PS_5X (X = Cl, Br, I). *J. Am. Chem. Soc.* **2017**, *139*, 10909−10918.

(17) Papakyriakou, M.; Lu, M.; Liu, Y.; Liu, Z.; Chen, H.; McDowell, M. T.; Xia, S. Mechanical behavior of inorganic lithium-conducting solid electrolytes. *J. Power Sources* **2021**, *516*, No. 230672.

(18) Yu, C.; van Eijck, L.; Ganapathy, S.; Wagemaker, M. Synthesis, structure and electrochemical performance of the argyrodite Li_6PS_5Cl solid electrolyte for Li-ion solid state batteries. *Electrochim. Acta* **2016**, *215*, 93−99.

(19) Rangasamy, E.; Liu, Z.; Gobet, M.; Pilar, K.; Sahu, G.; Zhou, W.; Wu, H.; Greenbaum, S.; Liang, C. An iodide-based $Li_7P_2S_8I$ superionic conductor. *J. Am. Chem. Soc.* **2015**, *137*, 1384−1387.

(20) Kang, J.; Han, B. First-principles characterization of the unknown crystal structure and ionic conductivity of $Li_7P_2S_8I$ as a Solid electrolyte for high-voltage Li-Ion batteries. *J. Phys. Chem. Lett.* **2016**, *7*, 2671−2675.

(21) Ando, K.; Matsuda, T.; Miwa, T.; Kawai, M.; Imamura, D. Degradation mechanism of all-solid-state lithium-ion batteries with argyrodite $Li_{7-x}PS_{6-x}Cl_x$ sulfide through high-temperature cycling test. *Battery Energy* **2023**, No. 20220052.

(22) Gil-González, E.; Ye, L.; Wang, Y.; Shadike, Z.; Xu, Z.; Hu, E.; Li, X. Synergistic effects of chlorine substitution in sulfide electrolyte solid state batteries. *Energy Storage Mater.* **2022**, *45*, 484−493.

(23) Gogia, A.; Wang, Y.; Rai, A. K.; Bhattacharya, R.; Subramanyam, G.; Kumar, J. Binder-free, thin-film ceramic-coated separators for improved safety of lithium-ion batteries. *ACS Omega* **2021**, *6*, 4204−4211.

(24) Wang, S.; Zhang, Y.; Zhang, X.; Liu, Ting.; Lin, Y-H.; Shen, Y.; Li, L.; Nan, C-W. High-conductivity argyrodite Li_6PS_5Cl solid electrolytes prepared via optimized sintering processes for all-solid-state lithium-sulfur batteries. *ACS Appl. Mater. Interfaces* **2018**, *10*, 42279−42285.

(25) Wang, Y.; Lu, D.; Xio, J.; He, Y.; Harvey, G. J.; Wang, C.; Zhang, J-G.; Liu, J. Superionic conduction and interfacial properties of the low temperature phase $Li_7P_2S_8$ $Br_{0.5}I_{0.5}$. *Energy Storage Mater.* **2019**, *19*, 80−87.

(26) Song, L.; Zheng, Y.; Xio, Z.; Wang, C.; Long, T. Review on thermal runaway of lithium-ion batteries of electric vehicles. *J. Electron. Mater.* **2022**, *51*, 30−46.

(27) Inoue, T.; Mukai, K. Are all-solid-state lithium-ion batteries really safe?-Verification by differential scanning calorimetry with an all-inclusive microcell. *ACS Appl. Mater. Interfaces* **2017**, *9*, 1507−1515.

(28) Ziv, B.; Haik, O.; Zinigrad, E.; Levi, M. D.; Aurbach, D.; Halalay, I. C. Investigation of graphite foil as current collector for positive electrodes of Li-Ion Batteries. *J. Electrochem. Soc.* **2013**, *160*, A581−A587.

(29) Liu, Q.; Liu, Y.; Jiao, X.; Song, Z.; Sadd, M.; Xu, X.; Matic, A.; Xiong, S.; Song, J. Enhanced ionic conductivity and interface stability of hybrid solid-state polymer electrolyte for rechargeable lithium metal batteries. *Energy Storage Mater.* **2019**, *23*, 105−111.

(30) Chen, S.; Che, H.; Feng, F.; Lio, J.; Wang, H.; Yin, Y.; Ma, Z-F. Poly(vinylene carbonate)-based composite polymer electrolyte with enhanced interfacial stability to realize high-performance room-temperature solid-state sodium batteries. *ACS Appl. Mater. Interfaces* **2019**, *11*, 43056−43065.
(31) Amatucci, G. G.; Tarascon, J. M.; Klein, L. C. Cobalt dissolution in $LiCoO_2$-based non-aqueous rechargeable batteries. *Solid State Ionics* **1996**, *83*, 167−173.
(32) Larsson, F.; Andersson, P.; Blomqvist, P.; Mellander, B. Toxic fluoride gas emissions from lithium-ion battery fires. *Sci. Rep.* **2017**, *7*, No. 10018.

https://doi.org/10.1021/acsomega.3c00261
ACS Omega 2023, 8, 12411−12417